Inorg. Chem. **2008**, *47*, 1496−1501

Inorganic Chemistry
Article

Vibrational Property Study of $SrGa_2H_2$ and $BaGa_2H_2$ by Inelastic Neutron Scattering and First Principles Calculations

Myeong H. Lee,[†] Michael J. Evans,[‡] Luke L. Daemen,[§] Otto F. Sankey,[†] and Ulrich Häussermann*,[‡]

Department of Physics, Arizona State University, P.O. Box 871504 Tempe, Arizona 85287-1504, Department of Chemistry and Biochemistry, Arizona State University, P.O. Box 871604, Tempe, Arizona 85287-1604, and Lujan Neutron Scattering Center, Los Alamos National Laboratory, P.O. Box 1663 Los Alamos, New Mexico 87545

Received September 28, 2007

Vibrational properties of the gallium hydrides $SrGa_2H_2$ and $BaGa_2H_2$ have been investigated by means of inelastic neutron scattering (INS) and first-principles calculations. The compounds contain Ga−H units being part of a two-dimensional polyanionic layer, $[(GaH)(GaH)]^{2-}$. The INS spectra are composed of dispersed internal Ga−H bending and stretching modes at frequencies above 600 cm^{-1} and external lattice modes at frequencies below 220 cm^{-1}. Frequencies of the internal modes are not susceptible to the metal countercation, indicating a strong integrity of the polyanionic layer as a building unit in the structures of $SrGa_2H_2$ and $BaGa_2H_2$. The Ga−H stretching modes have frequencies between 1200 and 1400 cm^{-1}, which is very low compared to molecular gallium hydrides. The weak Ga−H bond in $SrGa_2H_2$ and $BaGa_2H_2$ is balanced by Sr(Ba)−H interactions.

1. Introduction

Many metals and intermetallic compounds exhibit the ability to absorb and react with hydrogen. Metal hydride compounds can be polymeric, salt-like, or metallic materials, depending on the kind of metal involved and the preparation method applied. The many shapes of metal−hydrogen compounds have been puzzling for a very long time, and today there is still no conclusive understanding of the nature of the various metal/semimetal−hydrogen interactions and its consequences to chemical structures and physical properties.[1] Additional variation is provided by recently discovered polyanionic hydrides, which are obtained from the hydrogenation of Zintl phase precursors.[2–4] The peculiar feature of these hydrides is the incorporation of H in polymeric anions composed of p-block metal or semimetal atoms where it acts as a terminating ligand. This creates chemically new coordination environments for both metal and H atoms.

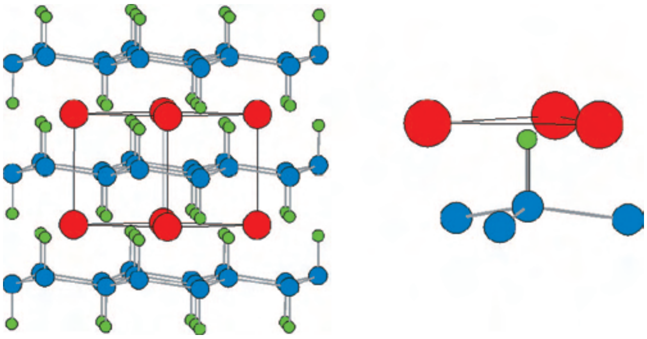
Figure 1. Crystal structure of $SrAl_2H_2$. Red, blue, and green circles denote Sr, Al, and H atoms, respectively. On the right-hand side, the local environment of an H atom is highlighted.

The prototype of a polyanionic hydride is $SrAl_2H_2$ which was discovered in 2000 by Gingl et al.[2] $SrAl_2H_2$ crystallizes with the trigonal space group $P\bar{3}m1$ and possesses a two-dimensional polyanion $[Al_2H_2]^{2-}$ in which Al atoms are arranged in puckered hexagon layers with the three nearest neighbors (Figure 1). The coordination of Al is completed by a hydrogen atom in a tetrahedral fashion, and $SrAl_2H_2$ appears charge-balanced when assigning the oxidation state −I for four-bonded Al and zero for singly bonded H. The

---

* To whom correspondence should be addressed. E-mail: ulrich.haussermann@asu.edu.

[†] Department of Physics.

[‡] Department of Chemistry and Biochemistry.

[§] Los Alamos National Laboratory.

(1) (a) Schlapbach, L., Ed.; *Topics in Applied Physics, Hydrogen in Intermetallic Compounds*; Springer: Berlin, 1992; Vol. *67*. (b) Wipf, H., Ed.; *Topics in Applied Physics, Hydrogen in Metals III*; Springer: Berlin, 1997; Vol. *73*.

(2) Gingl, F.; Vogt, T.; Akiba, E. *J. Alloys Compd.* **2000**, *306*, 127.

(3) Björling, T.; Noréus, D.; Häussermann, U. *J. Am. Chem. Soc.* **2006**, *128*, 817.

(4) Björling, T.; Noréus, D.; Jansson, K.; Andersson, M.; Leonova, E.; Edén, M.; Hålenius, U.; Häussermann, U. *Angew. Chem., Int. Ed.* **2005**, *44*, 7269.

10.1021/ic7019318 CCC: $40.75

H-terminated puckered hexagon nets are stacked in the same orientation on top of each other in the *c* direction. Sr atoms are sandwiched between two triangles of H atoms in a D_{3d} staggered way. Although $SrAl_2H_2$ is formally charge balanced, its electronic structure does not display a true band gap at the Fermi level but a pronounced pseudo gap, and the compound should be a metallic conductor.[5,6]

The bonding properties and lattice dynamics of polyanionic hydrides are virtually unexplored; however, their knowledge would provide valuable insight into the fundamental question of how hydrogen interacts with metals and semimetals.[7] Recently we performed a comparative vibrational property study of $SrAl_2H_2$ and isoelectronic SrAlSiH, which is a semiconductor, and found unexpectedly low frequencies for the stretching mode of the [Al−H] entities occurring in both compounds.[5] In this paper we report on the vibrational properties of $SrGa_2H_2$ and $BaGa_2H_2$, which are structure analogues to $SrAl_2H_2$ and contain two-dimensional $[Ga_2H_2]^{2-}$ polyanions.[3]

Inelastic neutron scattering (INS) is the method of choice to obtain vibrational spectra of hydrogen containing systems.[8–11] This is especially the case for metallic conducting materials where, for example, IR spectroscopy cannot be applied. Further, in INS, unlike optical spectroscopy, the intensity does not depend on electronic properties such as dipole moment or polarizability. Thus, there are no symmetry-based selection rules and all modes are allowed. The intensity of modes is proportional to the amplitude of motion (displacement) and scattering cross section of atoms involved. Compared to all other elements, the cross section of hydrogen is extremely large which makes INS a superb probe for investigating hydrogen motion. Another important feature with INS is the simplicity of the neutron−nucleus interaction, which allows one to quantitatively calculate a neutron vibrational spectrum for a known structure on the basis of frequencies and displacements obtained from first principles methods and compare directly the calculated spectrum with the observed data.[12,13] Such quantitative agreement is difficult to achieve for optical spectroscopies. Although first principles calculations of phonons (frequencies and displacements) either are computationally demanding ("direct method" approach)[14,15] or have been requiring new codes (linear response approach),[16,17] it is nowadays possible to obtain reliable results within the quasiharmonic approximation in a fairly routine manner.[18–20] The combined application of INS spectroscopy and theoretical modeling is synergetic and has become the state-of-the-art procedure for studying the vibrational properties of molecules and solids: computational modeling ensures the proper assignment of modes and interpretation of experimental spectra, and vice versa, experimental spectra serve to assess the quality of computed phonon density of states and dispersions curves, thus validating the applied computational method and involved approximations.[21,22]

2. Experimental and Computational Details

All steps of the synthesis were carried out under dry argon. Sr (99.95% purity), Ba (99.9%), and Ga (99.999%) were purchased from Alfa Aesar. The starting materials $SrGa_2$ and $BaGa_2$ were prepared from stoichiometric ratios of the pure elements. The elemental mixtures were loaded into Ta ampoules, which were placed in fused silica Schlenk tubes under reduced pressure. The mixtures were heated at 200 K/h to 800 °C, held there for 24 h, and then cooled at 100 K/h to room temperature. To obtain $SrGa_2H_2$ and $BaGa_2H_2$, the binary starting materials were ground into powders and pressed into pellets. The pellets were loaded in corundum crucibles, which were placed into stainless steel autoclaves. Hydrogenation was carried out at 200 °C for 3 days and a hydrogen pressure of 50 bar.

For INS spectroscopy, the hydride samples were loaded into an aluminum sample holder under a He atmosphere. The sample holder was subsequently sealed and mounted in a cryostat. The spectra of the two hydrides were measured at 10 K on the filter difference spectrometer (FDS) instrument at the Lujan Center at Los Alamos National Laboratory. Data were treated by deconvolution of the instrumental resolution function. The two main algorithms used for FDS include a discrete, direct deconvolution[23] or the use of Bayesian methods (Maximum Entropy).[24] Both methods are robust, with the first technique providing an energy resolution of the order of 4–5%, whereas Maximum Entropy (ME) is capable of reconstructing a vibrational spectrum with an energy resolution of the order of 2–3% and is useful to help resolve overlapping peaks or fainter features such as shoulders. However, the higher resolution achieved with ME comes sometimes at the price of spurious small intensity wiggles.

---

(5) Lee, M. H.; Sankey, O. F.; Björling, T.; Moser, D.; Noréus, D.; Parker, S. F.; Häussermann, U. *Inorg. Chem.* **2007**, *46*, 6987.

(6) Orgaz, E.; Aburto, A. *Int. J. Quantum Chem.* **2005**, *101*, 783.

(7) Züttel, A. *Naturwissenschaften* **2004**, 91.

(8) Mitchell, P. C. H.; Parker, S. F.; Ramirez-Cuesta, A. J.; Tomkinson, J. *Vibration Spectroscopy with Neutrons - With Applications in Chemistry, Biology, Materials Science and Catalysis*, Series on Neutron Techniques and Applications; Vol. *3*; World Scientific: Hackensack NJ, 2005.

(9) Hudson, B. S. *Vib. Spectrosc.* **2006**, *42*, 25.

(10) Kearley, G. *J. Spectrochim. Acta* **1992**, *48A*, 349.

(11) Kearley, G. J. *Nucl. Instrum. Methods Phys. Res., Sect. A* **1995**, *354*, 53.

(12) Parker, S. F.; Bennington, S. M.; Ramirez-Cuesta, A. J.; Auffermann, G.; Bronger, W.; Herman, H.; Williams, K. P. J.; Smith, T. *J. Am. Chem. Soc.* **2003**, *125*, 11656.

(13) Parker, S. F.; Refson, K.; Williams, K. P. J.; Braden, D. A.; Hudson, B. S.; Yvon, K. *Inorg. Chem.* **2006**, *45*, 10951.

(14) Kresse, G.; Furthmüller, J.; Hafner, J. *Europhys. Lett.* **1995**, *32*, 729.

(15) (a) Palinski, K.; Li, Z.-Q.; Kawazoe, Y. *Phys. Rev. Lett.* **1997**, *78*, 4063. (b) Parlinski, K.; Li, Z.-Q.; Kawazoe, Y. *Phys. Rev. Lett.* **1998**, *81*, 3298.

(16) Savrasov, S. Y. *Phys. Rev. B* **1996**, *54*, 16470.

(17) Baroni, S.; de Gironcoli, S.; Dal Corso, A. *Rev. Mod. Phys.* **2001**, *73*, 515.

(18) (a) Colognesi, D.; Barrera, G.; Ramirez-Cuesta, A. J.; Zoppi, M. *J. Alloys Compd.* **2007**, *427*, 18. (b) Wu, H.; Zhou, W.; Udovic, T. J.; Rush, J. J.; Yidirim, T. *J. Alloys Compd.* **2007**, *436*, 51.

(19) (a) Peles, A.; Chou, M. Y. *Phys. Rev. B* **2006**, *73*, 184302. (b) Majzoub, E. H.; McCarty, K. F.; Ozolins, V. *Phys. Rev. B* **2005**, *71*, 024118.

(20) Schimmel, H. G.; Johnson, M. R.; Kearley, G. J.; Ramirez-Cuesta, A. J.; Huot, J.; Mulder, F. M. *Mater. Sci. Eng., B* **2004**, *108*, 38.

(21) Barrera, G. D.; Colognesi, D.; Mitchell, P. C. H.; Ramirez-Cuesta, A. J. *Chem. Phys.* **2005**, *317*, 119.

(22) Verdal, N.; Rivera, S. A.; Hudson, B. S. *Chem. Phys. Lett.* **2007**, *437*, 38.

(23) (a) Taylor, A. D.; Wood, E. J.; Goldstone, J. A.; Eckert, J. *Nucl. Instrum. Methods Phys. Res.* **1994**, *221*, 408. (b) Mezei, F.; Vorderwisch, P. *Physica B* **1989**, *156 & 157*, 678. (c) Litvinenko, E. I.; Zhidkov, E. P. *Comput. Phys. Commun.* **2000**, *127*, 229.

(24) Sivia, D. S. *Data Analysis - A Bayesian Tutorial*; Oxford University Press: Oxford, 1996.

Table 1. Computationally Relaxed Structural Parameters for $SrGa_2H_2$ and $BaGa_2H_2$ (Space Group $P\bar{3}m1$) Compared with Experimental Parameters[a]

$SrGa_2H_2$	theory (PP-GGA)	exptl (ref 3)
a (Å)	4.4061	4.4010(4)
c (Å)	4.7304	4.7109(4)
Ga (1/3,2/3,z)	0.4668	0.4656(7)
H (1/3,2/3,z)	0.1042	0.1067(8)
$BaGa_2H_2$	theory (PP-GGA)	exptl (ref 3)
a (Å)	4.5729	4.5334(6)
c (Å)	5.0233	4.9069(9)
Ga (1/3,2/3,z)	0.4719	0.4680(4)
H (1/3,2/3,z)	0.1312	0.1232(4)

[a] For $SrAl_2H_2$ see ref 5.

Table 2. Important Interatomic Distances (Å) in $SrGa_2H_2$, $BaGa_2H_2$, and $SrAl_2H_2$[a]

		$SrAl_2H_2$[b]	$SrGa_2H_2$[c]	$BaGa_2H_2$[c]
Ae−H	6x	2.653(1) *2.654*	2.586(1) *2.591*	2.683(1) *2.721*
E−H	1x	1.706(4) *1.716*	1.687(5) *1.715*	1.689(3) *1.711*
E−E	3x	2.641(1) *2.634*	2.557(1) *2.563*	2.633(4) *2.655*
H−H	3x	2.770(1) *2.772*	2.727(3) *2.728*	2.880(2) *2.951*

[a] Values from computationally relaxed structures are in italics. [b] Experimental values from ref 2; computational values from ref 5. [c] Experimental values from ref 3; computational values from this work.

Theoretical calculations were performed using density functional theory with a planewave basis set and pseudopotential. The VASP[25] code was used for this purpose. We used the generalized gradient approximation (GGA) of Perdew and Wang[26] to approximate the exchange-correlation energy. Ultrasoft pseudopotentials were used[27] to consider only the valence electrons in the calculations and not the core electrons. For Sr and Ba, semicore p electrons were also included. The lattice parameters and the ionic positions were optimized for a fixed volume of the unit cell, and this process was repeated for several volumes. The equation of state was obtained, and the optimized lattice constants were determined from the global minimum energy. For optimized cell parameters, the internal coordinates of the unit cell were reoptimized to have zero-force. The Brillouin zone integration was performed over a 10 × 10 × 10 Monkhorst-Pack grid.[28] The relaxed structural parameters are shown in Table 1.

The phonon vibrational modes were determined using a direct method[15] with supercells. In the direct method, one column of the dynamical matrix is obtained from the forces when a single atom is displaced by a finite displacement from its equilibrium position. The force is divided by the displacement to give a column of the force constant matrix. A 3a × 3a × 3c supercell was generated, and the position of all the atoms in the supercell was reoptimized using a 3 × 3 × 3 k-point sampling until the forces converged to less than 0.1 meV/ Å. Each atom in the supercell was displaced by 0.01 Å along each of the Cartesian directions, and the Hellmann–Feynman force on each atom was obtained. The number of atoms displaced was reduced by considering the symmetry. To remove cubic anharmonicity, the displacement of each atom was repeated in both the positive and negative directions, and the spring constants were averaged. We assumed a finite range of interaction (less than half the supercell dimensions) to obtain the wavevector dependent dynamical matrix. Normal mode frequency and eigenvectors were obtained by diagonalizing the wavevector-dependent dynamical matrix and used to compute the INS spectra by the aCLIMAX program.[29]More details of phonon frequency calculations can be found in ref 30. To make previous work compatible with the present calculation, we recomputed the phonon dispersion curve for $SrAl_2H_2$ with a 3a × 3a × 3c supercell reoptimized using a 3 × 3 × 3 k-point sampling. The present phonon dispersion curve remained almost the same as in the previous calculation,[5] which was performed using a 2 × 2 × 2 k-point sampling.

3. Results

$SrGa_2H_2$ and $BaGa_2H_2$ crystallize with the trigonal $SrAl_2H_2$ structure (Figure 1). Important interatomic distances are compiled in Table 2. Remarkably, the Ga−H distance in $SrGa_2H_2$ and $BaGa_2H_2$ is virtually identical (1.69 Å), and this distance is very similar to the Al−H distance in $SrAl_2H_2$ (1.71 Å). Both metal−H distances are relatively large compared to terminal Al−H and Ga−H bond lengths in molecular species EH_n (E = Al, Ga; n = 1, 2, 3)[32–35] or in tetrahedral complexes EH_4^- occurring in alkali metal (A) Al and Ga hydrides (AEH_4).[36,37] Hydrogen atoms are coordinated by one E and three alkaline earth (Ae) metal atoms; E atoms are coordinated by one H and three further E atoms; and Ae atoms are coordinated distorted octahedrally by six H atoms. The E−E distances in AeE_2H_2 are in a range typically observed for Zintl phases containing polyanions with E−E single bonds; note, however, the widening of the Ga−Ga bond length when going from $SrGa_2H_2$ to $BaGa_2H_2$. Also Sr−H distances appear flexible and shrink from 2.65 to 2.59 Å when going from $SrAl_2H_2$ to $SrGa_2H_2$. In binary SrH_2 and BaH_2 with the cotunnite ($PbCl_2$) structure, Ae atoms are coordinated by nine H atoms forming distorted tricapped trigonal prisms, with distances ranging from 2.43 to 2.81 Å and 2.57 to 2.92 Å for SrH_2 and BaH_2, respectively.[38,39]

The INS spectra of $SrGa_2H_2$ and $BaGa_2H_2$ are shown in Figure 2 for the ranges between 500 and 2900 cm^{-1} and 70 and 250 cm^{-1} (insets). Both spectra are characterized by high intensity bands centered around 800 and 1350 cm^{-1} and associated overtones above 1500 cm^{-1}. The band around 800 cm^{-1} appears split. High intensity bands imply H motion

---

(25) (a) Kresse, G.; Furthmüller, J. *J. Phys. Rev. B* **1996**, *54*, 11169. (b) Kresse, G.; Furthmüller, J. *Comput. Mater. Sci.* **1996**, *6*, 15. (c) Kresse, G.; Hafner, J. *Phys. Rev. B* **1993**, *47*, 558.

(26) Perdew, J. P.; Wang, Y. *Phys. Rev. B* **1992**, *45*, 13244.

(27) Vanderbilt, D. *Phys. Rev. B* **1990**, *41*, 7892.

(28) Monkhorst, H. J.; Pack, J. D. *Phys. B* **1976**, *13*, 5188.

(29) (a) Ramirez-Cuesta, A. J. *Comput. Phys. Commun.* **2004**, *157*, 226. (b) Champion, D.; Tomkinson, J.; Kearley, G. *Appl. Phys. A: Mater. Sci. Process.* **2002**, *74*, S1302.

(30) (a) Dong, J.-J.; Sankey, O. F. *J. Phys.: Condens. Matter* **1999**, *11*, 6129. (b) Dong, J.-J.; Sankey, O. F. *J. Appl. Phys.* **2000**, *87*, 958. (c) Nolas, G. S.; Kendziora, C. A.; Gryko, J.; Dong, J.; Myles, C.; Poddar, A.; Sankey, O. F. *J. Appl. Phys.* **2002**, *92*, 7225.

(31) The Cartesian k-points A, L, M, Γ, H, and K are $(2\pi/c)(0,0,1/2)$, $(2\pi/a)(1/2,\sqrt{3}/6,a/2c)$, $(2\pi/a)(1/2,\sqrt{3}/6,0)$, $(0,0,0)$, $(2\pi/a)(2/3,0,a/2c)$, and $(2\pi/a)(2/3,0,0)$, respectively.

(32) Aldridge, S.; Downs, A. J. *Chem. Rev.* **2001**, *101*, 3305.

(33) Ito, F.; Nakanaga, T.; Takeo, H.; Jones, H. *J. Mol. Spectrosc.* **1994**, *164*, 379.

(34) Pullumbi, P.; Mijoule, C.; Manceron, L.; Bouteiller, Y. J. *Chem. Phys.* **1994**, *185*, 13.

(35) Pullumbi, P.; Bouteiller, Y.; Manceron, L.; Mijoule, C. *Chem. Phys.* **1994**, *185*, 25.

(36) Iniguez, J.; Yildirim, T.; Udovic, T. J.; Sulic, M.; Jensen, C. M. *Phys. Rev. B* **2004**, *70*, 060101(R).

(37) Irodova, A. V.; Somenkov, V. A.; Bakum, Si. I.; Kuznetsova, S. F. *Z. Phys. Chem. Neue Fol.* **1989**, *163*, 239.

(38) Brese, N. E.; O'Keeffe, M.; von Dreele, R. B. *J. Solid State Chem.* **1990**, *88*, 571.

(39) Bronger, W.; Chi, C. S.; Mueller, P. *Z. Anorg. Allg. Chem.* **1987**, *545*, 69.

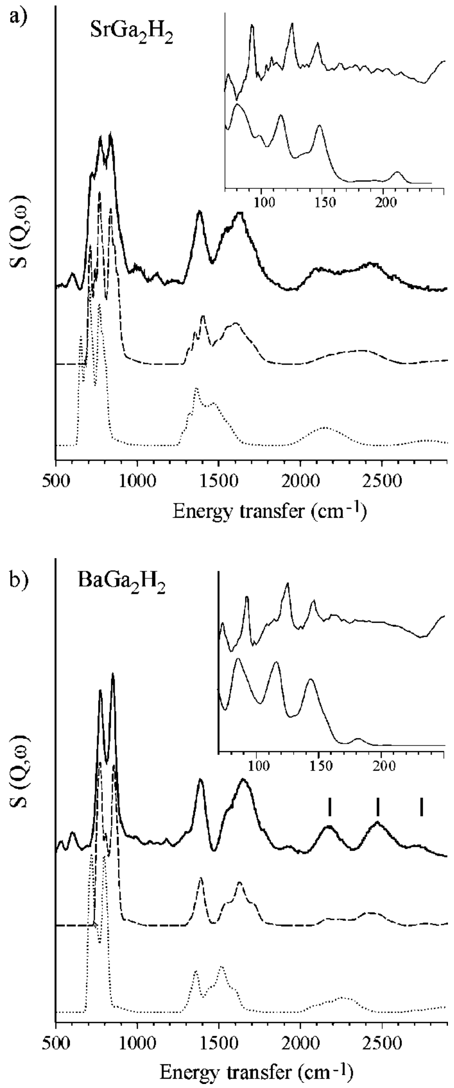

Figure 2. Measured (solid line) and calculated (broken and dotted lines) INS spectrum of $SrGa_2H_2$ (a) and $BaGa_2H_2$ (b). The calculated spectra are based on frequencies and displacements obtained from first principles phonon calculations. For spectra represented with broken lines, frequencies of external fundamentals have been scaled to match the experimental ones, while those represented with dotted lines were obtained with the original frequencies. In the spectra calculations, overtones and combinations up to three quanta are included. Vertical markers in (b) indicate the locations of maxima from the combination, 0–3 bending, and 0–2 stretching modes. The insets show the internal modes at low frequency (solid line - experimental spectrum, dotted line - calculated spectrum). Extra intensities in the experimental spectra (between 500 and 650 cm^{-1}, 900 and 1200 cm^{-1}, and around 1900 cm^{-1}) are spurious peaks introduced by the Maximum Entropy method used for deconvoluting the spectrometer data (see Supporting Information).

and, as we will see later, correspond to [Ga−H] bending and stretching modes. The dispersion implies that H atoms from neighboring unit cells, which is primarily between polyanionic layers, interact. The energy of a vibration excited in the crystal depends then on its wavevector (momentum) k. The Γ point ($k = 0$) corresponds to the situation where atoms displace identically in all unit cells and is observed with optical spectroscopy (no momentum transfer). Apart from vibrations stemming from H, there are modes in $AeGa_2H_2$ where mainly Ga or Ae displacements are involved. The bands arising from such modes have much lower intensity and appear at lower frequency compared to the H modes. Although compounds $AeGa_2H_2$ represent solid state crystalline systems, it is then convenient to classify H based modes as internal modes and the remaining ones as external (lattice) modes, in analogy to molecular systems.[12,13]

Table 3. Calculated Phonon Frequencies (in cm^{-1}) for Optical Modes at the Γ Point (Equilibrium Lattice Parameters)

mode type	$SrGa_2H_2$	$BaGa_2H_2$	$SrAl_2H_2$
A_{2u} (Ae)	104	99	141
E_u (Ae)	112	101	144
A_{1g} (E−E out-of-plane)	160	161	251
E_g (E−E in-plane stretch)	216	188	353
E_u (E−H bend)	638	689	565
E_g (E−H bend)	814	826	752
A_{2u} (E−H stretch)	1254	1275	1288
A_{1g} (E−H stretch)	1363	1375	1356

Pivotal for the interpretation of the INS spectra is the correct assignment of modes. For this, results from first principles calculations are invaluable, and usually analysis of the situation at the Γ point is sufficient. Table 3 shows calculated frequencies at the Γ point, including those for $SrAl_2H_2$, and Figure 3 sketches the displacements of the high frequency modes. There are five atoms in the primitive unit cell of the $SrAl_2H_2$ structure type which give rise to 15 normal modes of vibrations. In addition to the acoustic modes (3), there are twelve optic modes, which occur as four pairs (A + E). The symbols A and E denote generically the main displacements along z and in-plane xy, respectively. At Γ, the high frequency vibrations (between 600 and 1400 cm^{-1}) correspond to the (internal) [Ga−H] vibrations which are composed of two stretching (A_{1g} and A_{2u}) and two degenerate bending modes (E_g and E_u) (cf. Figure 3). These modes are well separated from the six external lattice modes (Ga atoms displaced along z in opposite directions (A_{1g}) and in-plane Ga−Ga stretching (E_g); Ae vibrations against (A_{2u}) and along puckered nets (E_u)), which have frequencies below 220 cm^{-1}.

Returning to the INS spectra (Figure 2), we can now assign the bands around 800 and 1350 cm^{-1} to dispersed [Ga−H]

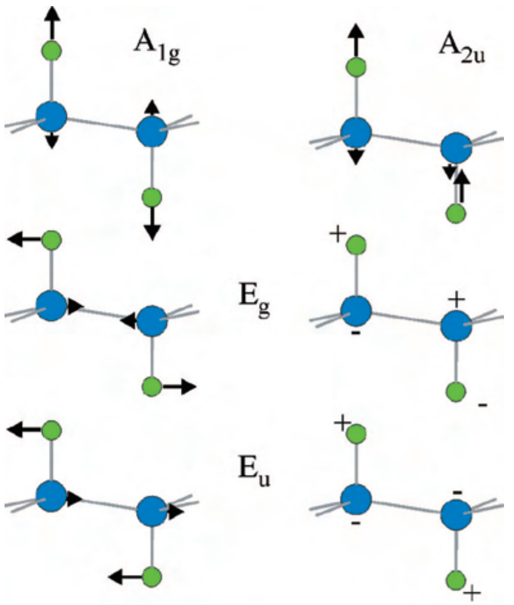

Figure 3. Approximate displacement vectors for the external modes in compounds with the $SrAl_2H_2$ structure.

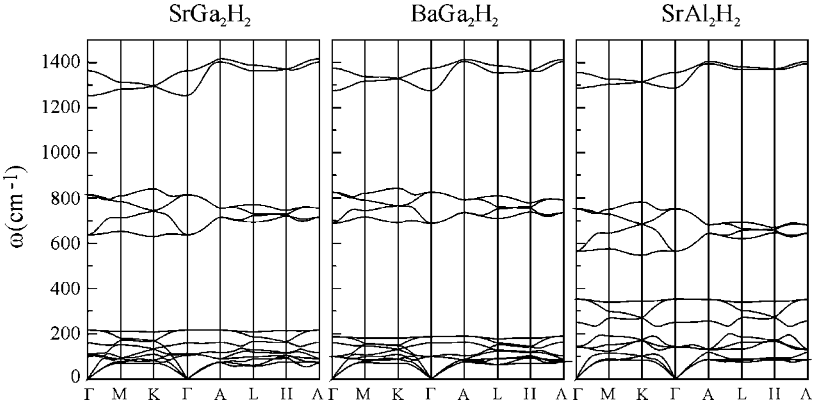

Figure 4. Calculated phonon dispersion curves for $SrGa_2H_2$ (left), $BaGa_2H_2$ (middle), and $SrAl_2H_2$ (right) for the symmetry points of the Brillouin zone.[31]

bending and stretching modes, respectively. Spectral intensities above 1500 cm^{-1} are due to overtones and combinations. The bending modes produce a 0–2 overtone band which adjoins to the [Ga−H] stretching band. In the spectrum of $SrGa_2H_2$ (Figure 2a), this overtone and the stretching fundamental overlap partly, while for $BaGa_2H_2$ they are rather well separated. Additionally, two quanta events are the combination mode and stretching mode overtone. Again, these features appear much better resolved for $BaGa_2H_2$ (at around 2100 and 2700 cm^{-1}, respectively (Figure 2b)). However, the stretching mode 0–2 overtone is very difficult to detect. More pronounced, at least for $BaGa_2H_2$, is the three quanta overtone band from the bending mode (at around 2400 cm^{-1}). Turning to the external modes, three bands can be discerned in the experimental spectra between 90 and 200 cm^{-1} (Ae in-plane and out-of-plane, and Ga−Ga out-of-plane). The Ga−Ga in-plane stretching mode has the highest frequency (around 200 cm^{-1}) but attains a very low intensity and is not really visible in the spectra (Figure 2, insets).

Finally, the INS spectra of $AeGa_2H_2$ were calculated by employing computed frequencies and displacements across the Brillouin zone (i.e., considering the phonon dispersion of modes) and taking into account 0–1 to 0–3 transitions. The agreement with the experimental spectrum is satisfactory (Figure 2). In the calculated spectrum, the bands of internals are split according to their modes. This feature is not well resolved in the experimental spectra, apart from the split of E_g and E_u based modes in the band of bending modes. The most apparent discrepancy between calculated and experimental spectra is the underestimation of the frequencies of the [Ga−H] bending modes (by about 9%) which in turn causes a very high overlap of the bending mode overtones with the stretching mode. When shifting the first principles frequencies of the [Ga−H] fundamentals to match the ones in the experimental spectrum and subsequently recalculating the INS spectrum, excellent agreement between calculated and experimental spectra is achieved. This scaling procedure is frequently performed because frequencies from first principle calculations will hardly coincide with experimental ones.[8,29] The reasons can be manifold and ground in the approximations applied for calculating phonons.[14–17,30] Note that, e.g., calculated phonon frequencies are very sensitive to lattice parameters, and small changes in axial ratios can introduce significant changes to the lattice dynamics.[40]

4. Discussion

The INS spectra of the two alkaline earth gallium hydrides $SrGa_2H_2$ and $BaGa_2H_2$ are very similar and also resemble closely that for $SrAl_2H_2$.[5] Comparing $SrGa_2H_2$ with $SrAl_2H_2$ allows us to discuss differences of vibrational properties between the polyanions $[Al_2H_2]^{2-}$ and $[Ga_2H_2]^{2-}$, while a comparison of $SrGa_2H_2$ with $BaGa_2H_2$ allows us to discuss the influence of the countercation on the vibrational properties of $[Ga_2H_2]^{2-}$. For these discussions, we will refer to the calculated phonon dispersion curves compiled in Figure 4. These dispersion curves show the phonon frequencies along special directions in the hexagonal Brillouin zone. *k* points describe the propagation direction and the modulation of displacements of a phonon.[41] The degeneracy of modes at Γ (cf. Table 2) - and other high-symmetry points - is removed at a general *k* point. The dispersion width of a mode relates to the broadness of the corresponding band in the INS spectrum, which can be considered as an experimentally determined phonon density of states.

In the three $SrAl_2H_2$-type compounds, hydrogen is bonded terminally to Al or Ga. The fundamental stretching modes are then a direct measure of the E−H bond strength. The two stretching modes disperse virtually over the same range of frequencies for all three compounds (1200–1400 cm^{-1}). From this, we can conclude that H is equally strongly bonded to Al and Ga, which resembles the situation in molecular entities EH, EH_2 (C_{2v}), and EH_3 (D_{3h}) where stretching frequencies (and E−H distances) are very similar for corresponding pairs AlH_n/GaH_n ($n = 1$: $r_e \approx 1.65$ Å, $\omega_e \approx 1650$ cm^{-1}; $n = 2$: $r_e \approx 1.60$ Å, $\omega_e \approx 1800$ cm^{-1}; $n = 3$: $r_e \approx 1.57$ Å, $\omega_e \approx 1900$ cm^{-1}).[32–35,42] However, the stretching modes of terminally bonded E−H entities in polyanions $[E_2H_2]^{2-}$ are at very low wavenumbers, which implies that H is actually rather weakly bonded to E. This observation appears surprising at first sight since these E−H bonds

---

(40) Kearley, G. J.; Johnson, M. R.; Tomkinson, J. *J. Chem. Phys.* **2006**, *124*, 044514.

(41) Dove, M. T. *Introduction to Lattice Dynamics*; Cambridge University Press: Cambridge, 1993.

(42) Wang, X.; Andrews, L. *J. Phys. Chem. A* **2003**, *107*, 11371.

formally correspond to single bonds. Considering the further coordination of H in AeE_2H_2 by triangularly arranged Ae atoms (or formally Ae^{2+} ions) bears an explanation (cf. Figure 1): Ae−H interactions will compete with the E−H interaction and elongate the E−H bond length (to about 1.7 Å) with respect to the equilibrium distance of molecular EH (around 1.65 Å).

The bending modes, where H displaces toward Ae atoms, reflect indirectly the strength of Ae−H interactions and will stiffen (i.e., shift to higher frequencies) for stronger Ae−H interactions. These modes appear in a range between 630 and 830 cm^{-1} for $SrGa_2H_2$ but between 560 and 750 cm^{-1} for $SrAl_2H_2$. This implies that Sr−H interactions are stronger in $SrGa_2H_2$ compared to $SrAl_2H_2$. The higher bending mode frequencies are also reflected in the shorter Sr−H distance in $SrGa_2H_2$ compared to $SrAl_2H_2$ (2.65 vs 2.59 Å). Ga−H bending mode frequencies are very similar for $SrGa_2H_2$ and $BaGa_2H_2$ suggesting that Sr−H and Ba−H interactions are equally strong in these two hydrides.

Turning to the external modes, the most interesting ones are those which involve displacements of covalently bonded E atoms within the polyanion (E atoms displaced along z in opposite directions (type A) and in-plane E−E stretching (type E)). These modes appear between 280 and 380 cm^{-1} for $SrAl_2H_2$ and are clearly separated from the lower frequency Sr and acoustic modes. For the $AeGa_2H_2$ compounds, the E−E modes are at considerably lower frequencies. However, this drop of frequencies is mainly due to the atomic mass increase of E. The ratio $\sqrt{m_{Al}}/\sqrt{m_{Ga}} \approx 0.6$ corresponds quite precisely to the ratio of E−E mode frequencies in $SrAl_2H_2$ and $SrGa_2H_2$ (cf. Table 2). Thus Al−Al and Ga−Ga force constants are very similar in SrE_2H_2. In $BaGa_2H_2$, the Ga−Ga distance is elongated compared to $SrGa_2H_2$ and the frequency of the in-plane stretching mode is lower by about 10%, which implies a slightly weaker Ga−Ga bond. Structures and bonding properties of polyanions in Zintl phases are likened to isoelectronic neutral arrangements.[43,44] However, the strength of element−element bonds in polyanions is much weaker than in corresponding isoelectronic neutral systems involving elements with a higher atomic number from the same period. Formally, $[Al_2H_2]^{2-}$ and $[Ga_2H_2]^{2-}$ would be isoelectronic (and isostructural) to layered polysilane $(SiH)_n$ and polygermane $(GeH)_n$, respectively. However, these compounds cannot be obtained in a pure form and are not well characterized.[45] To relate the strength of covalent E−E bonds in polyanions of AeE_2H_2, we may simply compare with elemental silicon and germanium (similar "sp^3"-like bonding situation for E and similar atomic masses). Here the frequencies of the optic phonons at $k = 0$ are 521 and 303 cm^{-1}, respectively.[46]

5. Conclusions

Polyanionic hydrides offer new coordination environments for metal and H atoms. In particular, in the isostructural compounds $SrAl_2H_2$, $SrGa_2H_2$, and $BaGa_2H_2$ (AeE_2H_2), H is terminating puckered hexagon nets of formally −1 charged four-bonded Al and Ga atoms to yield two-dimensional polyanions $[E_2H_2]^{2-}$. However, the charge assignment according to the Zintl concept (i.e., $[E^{1-}\cdot\cdot H]$) is not reflecting the actual charge distribution in systems AeE_2H_2 where H is the most electronegative component. The other border case is hydridic hydrogen binding datively to E (i.e., $[E \leftarrow H^{1-}]$).

The vibrational properties of $SrGa_2H_2$ and $BaGa_2H_2$ were characterized by a combined inelastic neutron scattering and computational study and compared with those of $SrAl_2H_2$. The exchange of Sr for heavier and larger Ba in $AeGa_2H_2$ leads structurally to a larger separation of polyanionic $[Ga_2H_2]^{2-}$ layers and elongated Ga−Ga distances. The larger separation of layers has virtually no consequences to vibrations involving H; however, the covalent Ga−Ga bond is weaker in $BaGa_2H_2$ as expressed by a lower in-plane stretching frequency. Compared to molecular entities EH_n ($n = 1, 2, 3$), the bond strength of E−H in $[E_2H_2]^{2-}$ is clearly weaker as indicated in the low frequencies of the stretching mode. This phenomenon is attributed to the effective coordination of H by Ae in the solid state polyanionic hydrides and demonstrates the complex interplay of different metal−H interactions in multinary metal hydride systems.

Acknowledgment. This work has been supported by National Science Foundation grant DMR-0638826 and has made use of the Manuel Lujan, Jr. Neutron Scattering Center at Los Alamos National Laboratory, which is funded by the Department of Energy's Office of Basic Energy Sciences. Los Alamos National Laboratory is operated by Los Alamos National Security, LLC, under DOE Contract DE-AC52-06NA25396.

Supporting Information Available: INS spectra obtained by discrete, direct, deconvolution of the spectrometer raw data (Figure S1). This material is available free of charge via the Internet at http://pubs.acs.org.

IC7019318

---

(43) Müller, U. *Inorganic Structural Chemistry*; 2nd ed.; Wiley: New York, 1993.

(44) Kauzlarich, S. A., Ed.; *Chemistry, Structure and Bonding of Zintl Phases and Ions*; VCH: New York, 1996.

(45) Wiberg, N., Ed.; *Holleman-Wiberg: Inorganic Chemistry*; Academic Press: San Diego, 2001.

(46) Menéndez, J. In *Raman Scattering in Materials Science*; Weber, W. H., Merlin, R., Eds.;Springer Series in Materials Science 42; Springer Verlag: Berlin, 2000; p 57.